Radiomics in the Differential Diagnosis of Glioblastoma under the Primary Neurooncoimaging Conditions

Nikita E. Maslov[1, 2], Daria A. Valenkova[3], Alexander M. Sinitca[3], Gennadiy E. Trufanov[1], Vladimir M. Moiseenko[2], Alexander Yu. Efimtsev[1], Vera V. Chernobrivtseva[1, 2]

[1]Almazov National Medical Research Centre, St. Petersburg, Russia;

[2]Saint Petersburg Clinical Scientific and Practical Center for Specialized Types of Medical Care (Oncological), St. Petersburg, Russia;

[3]Saint Petersburg Electrotechnical University "LETI", St. Petersburg, Russia

Abstract

Introduction. *According to the 2021 WHO Classification of Tumors of the Central Nervous System (CNS) and the 2023 Clinical Practice Guidelines on the Drug Management of Primary CNS Cancers, the first step of molecular genetic testing to identify the morphological type and malignancy of adult-type diffuse gliomas is the detection of isocitrate dehydrogenase (IDH) mutation status. However, tumor tissue biopsy as the conventional diagnostic standard has a number of limitations that can potentially be mitigated by applying the principles of radiomics to the interpretation of magnetic resonance (MR) images.*

*The **aim** of our study is to develop a radiomics model for IDH mutation status prediction, which can be applied to primary diagnostic imaging in patients with suspected adult-type diffuse gliomas.*

Materials and methods. *We conducted a retrospective comparative statistical analysis of radiomic features extracted from 46 conventional brain MR images of the patients with adult-type diffuse gliomas and identified IDH mutation status using the Random Forest algorithm of machine learning in combination with various preprocessing methods of the source imaging data and a semi-automated LevelTracing tool used for segmentation of the regions of interest (ROI).*

Results. *The most effective combination of tools for preprocessing, segmentation, and classification was found to be ScaleIntensity, LevelTracing, and Random Forest, respectively. Using this combination, we verified the reliability of six radiomic predictors identified at the previous study stage. These features were all associated with IDH mutation status, and most of them capture texture heterogeneity in the ROIs at the voxel level. We were also able to improve the prognostic performance of our classification model up to AUC = 0.845 ± 0.089 ($p < 0.05$).*

Conclusion. *Based on a small, technically heterogeneous sample of routine MR imaging data, we developed a multiparametric model of IDH mutation status prediction in the patients with adult-type diffuse gliomas. Our conclusion is that relatively uniform preprocessing techniques based on uniform voxel intensity changes, which allow to preserve the structural detail, are feasible in clinical practice. The identified radiomic, likely voxel-based, features reflect the severity of perifocal vasogenic edema and the measure of intratumor morphological heterogeneity. We plan to assess the reproducibility of the study results using similar medical imaging data from open sources and to develop a color mapping technique for the ROIs to facilitate visual interpretation of quantitative radiomic data.*

Keywords: *adult-type diffuse gliomas; morphological heterogeneity; radiogenomics; radiomics; MRI; IDH mutation status*

Ethics approval. The study was approved by the local Ethics Committee of the Almazov National Medical Research Centre (Protocol No. 10-22, October 3, 2022).

Source of funding. The authors did not receive support from any organization for the submitted work.

Conflict of interest. The authors declare that they have no apparent or potential conflicts of interest related to the publication of this article.

For correspondence: 2 Akkuratov st., St. Petersburg, Russia, 197341. Almazov National Medical Research Centre. E-mail: atickinwallsome@gmail.com. Nikita E. Maslov.

For citation: Maslov N.E., Valenkova D.A., Sinitca A.M., Trufanov G.E., Moiseenko V.M., Efimtsev A.Yu., Chernobrivtseva V.V. Radiomics in the differential diagnosis of glioblastoma under the primary neurooncoimaging conditions. *Annals of Clinical and Experimental Neurology.* 2025;19(1):30–42.

DOI: https://doi.org/10.17816/ACEN.1251

Received 17.12.2024 / Accepted 13.01.2025 / Published 30.03.2025

Радиомика в дифференциальной диагностике глиобластомы в условиях первичной нейроонковизуализации

Н.Е. Маслов[1, 2], Д.А. Валенкова[3], А.М. Синица[3], Г.Е. Труфанов[1], В.М. Моисеенко[2], А.Ю. Ефимцев[1], В.В. Чернобривцева[1, 2]

[1]Национальный медицинский исследовательский центр имени В.А. Алмазова, Санкт-Петербург, Россия;

[2]Санкт-Петербургский клинический научно-практический центр специализированных видов медицинской помощи (онкологический) имени Н.П. Напалкова, Санкт-Петербург, Россия;

[3]Санкт-Петербургский государственный электротехнический университет «ЛЭТИ», Санкт-Петербург, Россия

Аннотация

Введение. *Согласно классификации ВОЗ опухолей ЦНС 2021 г. и практическим рекомендациям по лекарственному лечению первичных опухолей ЦНС 2023 г., определение статуса изоцитратдегидрогеназы (IDH) является начальным этапом молекулярно-генетического тестирования при идентификации патоморфологических форм диффузных глиом взрослых. Однако традиционный диагностический стандарт, подразумевающий исследование биопсийного материала, обладает рядом ограничений, потенциально нивелируемых внедрением в алгоритм интерпретации традиционных магнитно-резонансных (МР) изображений принципов радиомики.*

Цель *исследования – разработка применимой в условиях первичных диагностических мероприятий радиомической модели прогнозирования IDH-статуса диффузных глиом взрослых.*

Материалы и методы. *Посредством применения метода машинного обучения Random Forest осуществляли ретроспективный сравнительный статистический анализ радиомических характеристик 46 традиционных МР-исследований головного мозга пациентов с диффузными глиомами взрослых и известным IDH-статусом в зависимости от вида предварительной обработки исходных данных визуализации с использованием полуавтоматизированного инструмента сегментации зон интереса LevelTracing.*

Результаты. *Установлена наиболее эффективная комбинация инструментов препроцессинга, сегментации и классификации – ScaleIntensity, LevelTracing и Random Forest соответственно. С её помощью верифицирована достоверность 6 выявленных на прошлом этапе исследования радиомических предикторов IDH-статуса, в большинстве являющихся характеристиками текстурной неоднородности зон интереса на воксельном уровне, а также увеличена прогностическая эффективность классификационной модели до AUC = 0.845 ± 0.089 ($p < 0.05$).*

Заключение. *Разработана мультипараметрическая предиктивная модель IDH-статуса при диффузных глиомах взрослых на основе рутинных данных МР-визуализации в условиях малой технически разнородной выборки. Сделан вывод о целесообразности использования относительно унифицированных методов предварительной обработки изображений, предполагающих равномерные изменения интенсивности вокселей с сохранной структурной детализацией. Выявленные радиомические характеристики, вероятно, на воксельном уровне иллюстрируют выраженность перифокального вазогенного отёка и феномена внутриопухолевой морфологической гетерогенности. Планируется оценка воспроизводимости полученных результатов на основе аналогичных данных медицинской визуализации из открытых источников, а также разработка методики цветового картирования зон интереса с целью привнесения элемента субъективного визуализационного анализа в процесс интерпретации количественных радиомических данных.*

Ключевые слова: *диффузные глиомы взрослых; морфологическая гетерогенность; радиогеномика; радиомика; магнитно-резонансная томография; IDH-статус*

Этическое утверждение. Исследование одобрено локальным этическим комитетом НМИЦ им. В.А. Алмазова (протокол № 10-22 от 03.10.2022).

Источник финансирования. Авторы заявляют об отсутствии внешних источников финансирования при проведении исследования.

Конфликт интересов. Авторы заявляют об отсутствии явных и потенциальных конфликтов интересов, связанных с публикацией настоящей статьи.

Адрес для корреспонденции: 197341, Россия, Санкт-Петербург, ул. Аккуратова, д. 2. НМИЦ им. В.А. Алмазова. E-mail: atickinwallsome@gmail.com. Маслов Н.Е.

Для цитирования: Маслов Н.Е., Валенкова Д.А., Синица А.М., Труфанов Г.Е., Моисеенко В.М., Ефимцев А.Ю., Чернобривцева В.В. Радиомика в дифференциальной диагностике глиобластомы в условиях первичной нейроонковизуализации. *Анналы клинической и экспериментальной неврологии.* 2025;19(1):30–42.

DOI: https://doi.org/10.17816/ACEN.1251

Поступила 17.12.2024 / Принята в печать 13.01.2025 / Опубликована 30.03.2025

Introduction

Glioblastoma tends to be found in older adults, rarely < 55 yo, with the highest incidence rates among all primary CNS malignancies of 48.6% (annual incidence rate: 3.2–3.4 per 100,000 population) [1]. One-year survival rate does not exceed 13%, even in patients aged 20–44 years [2]. Glioblastoma is the most aggressive type of brain tumor. In most cases, a patient dies within 14–16 months, assuming chemotherapy and radiotherapy treatment [3].

Up to 2021, the grading of gliomas was primarily based on histological features [4]. Currently, various biomarkers are used to derive additional information valuable for the diagnosis and prognosis of the disease and impacting the treatment planning.

The first basic molecular genetic markers of primary CNS tumors are mutations in the *IDH1/IDH2* genes and 1p/19q codeletion. Detecting these markers helps narrow down the differential diagnosis options and make a definitive diagnosis [5].

According to the 2021 WHO Classification of Tumors of the CNS, IDH-wildtype (*IDH*-WT) glioblastoma, IDH-mutant astrocytoma, and IDH-mutant/1p/19q-codeleted oligodendroglioma belong to the adult-type diffuse glioma family [6, 7].

The grading of gliomas is no longer strictly histological. Astrocytomas are now graded as CNS WHO grade 2, 3, or 4; oligodendrogliomas as CNS WHO grade 2, 3; and glioblastomas are assigned to CNS WHO grade 4. In the previous classification, the grading of gliomas was based predominantly on histological features such as necrosis, microvascular proliferation, nuclear atypia, etc., while the current 2021 WHO classification of tumors of the CNS mandates genetic testing of tumor tissue and prioritizes the identified genetic features in the differential diagnosis [8].

In the adult-type diffuse glioma family, only glioblastoma is characterized by the absence of IDH mutations. Mutation in the IDH genes is the key feature of molecular diagnostics for grade 2–4 adult-type diffuse gliomas and secondary glioblastomas (grade 1 gliomas have no mutations in the *IDH* genes) [8].

The minimum scope of diagnostic assessments for a suspected glial tumor includes a 3-plane brain MRI with standard MRI pulse sequences [8]. In routine clinical practice, the diagnostic use of these data is often limited to the identification of tumor location and size. However, rapid advances in radiogenomics over the past 15 years enabled expanding the potential use of MRI data to non-invasive prediction of molecular genetic characteristics of detected neoplasms.

Radiogenomics links radiomics, an original methodology that extracts and classifies digitized, predominantly textural features of a medical image, to molecular genetics, revealing statistically significant correlation between radiomic features unavailable at routine visual interpretation and histological and molecular characteristics of the tumor [9].

If radiomics models can reach an adequate level of predictive performance, the current diagnostic paradigm requiring tissue biopsy analysis will potentially be inferior to the radiomics-based neuro-oncology imaging in a number of factors. Conventional molecular genetic testing is incomparably time-consuming, which can adversely affect patient triage. At present, stereotactic needle biopsy is the least invasive method of diffuse and deep-brain tumor verification. It is still associated with numerous complications, with intracranial hemorrhage (in 5.8% of patients) being the most frequent and life-threatening of them [10]. In the case of intratumor heterogeneity, multiple biopsies may be required, often worsening the patient's condition, whereas radiomics approach allows non-invasive evaluation of the tumor substrate.

This advantage is also of great value for the treatment planning in patients who are ineligible for radical resection of the tumor or stereotactic needle biopsy due to contraindications to surgery or anesthesia, or when the tumor is located close to functionally significant regions of the brain [11]. In addition, virtual reality diagnostic tools are cost-effective [12].

The importance of radiogenomics approach in oncology, particularly the IDH mutation status prediction in glial tumors, has significantly increased over the past decade, especially in international contexts [13, 14]. However, the high-tech neuroimaging techniques employed in many studies are not available at the initial evaluation of a patient with suspected glioma [15, 16]. Moreover, the research in this area also aims at improving the predictive performance of the developed models, not only by focusing on specialized medical image data but also by testing various methods of image preprocessing, tools for extracting radiomic features, and methods for their statistical processing. The current trend is to include clinical and anamnestic data significantly correlated with a particular tumor type (age, gender, Karnofsky Performance Status, etc.) and even the elements of the radiologist's subjective interpretation into the datasets for the predictive model training [17, 18].

The choice of datasets for model development obviously requires standardization. Otherwise, optimistic theoretical results will be unreproducible and of limited use in routine diagnostic practice.

In the four years since the last revision of the 2021 WHO classification of tumors of the CNS, a number of studies published abroad presented results showing promising performance of the predictive models. W. Rui et al. developed a model for IDH mutation status prediction using T2-FLAIR and T1FS-CE MRI pulse sequences. However, to improve the model accuracy, they included data on quantitative susceptibility mapping (QSM) into the analysis. The ROC AUC score for the model based on T2-FLAIR and for the combination of T2-FLAIR, T1FS-CE, and QSM was 0.69 and 0.88, respectively [19]. S. Zhong et al. focused on the analysis of routine MRI pulse sequence data (T1, T1FS-CE, T2). However, they also used natural language processing (NLP) models based on semantic analysis of MRI reports and other documented clinical and anamnestic information. These data were subsequently processed and incorporated into the training datasets in order to purposely increase the model predictive performance (AUC = 0.98 for IDH-mutation status

Table 1. Distribution of tumors by morphological type, malignancy grade, and IDH mutation status

Diagnosis		*n*	%
Morphological type, malignancy grade	Glioblastoma G4	24	52.2
	Oligodendroglioma G3	7	15
	Astrocytoma G2	2	4.3
	Astrocytoma G3	5	11
	Astrocytoma G4	5	11
	Oligodendroglioma G2	3	6.5
IDH mutation status	WT	24	52
	M	22	48

prediction). In our opinion, such an approach makes this model somewhat useless in the third-party medical facilities using another natural language [18].

The quality of the extracted radiomic features depends significantly on the MR image preprocessing techniques [20]. Thus, at this stage, there is a need to develop radiomics-based models to predict IDH mutation status in the patients with adult-type diffuse glioma and to standardize this process to pursue the potential applicability of the results when using these models in primary differential diagnosis.

Our study considers the results obtained during its previous stage and continues the search for the most effective preprocessing tool and an optimal classification model [21, 22]. Noteworthy, a predictive model for IDH mutation status based on the updated 2021 WHO classification of tumors of the CNS allows to rule out an entire morphologic type of tumor in a non-invasive manner already at the initial stage of the differential diagnosis: namely, primary glioblastoma IDH-WT, which is characterized by an almost twice worse prognosis compared to the IDH-M entity and by a poor response to radio- and chemotherapy [8].

The **aim** of our study is to develop a radiomics model for IDH mutation status prediction, which can be applied to primary diagnostic imaging in patients with suspected adult-type diffuse gliomas.

Materials and methods

We retrospectively analyzed primary brain MRI data yielded from 46 patients aged 18–84 years with adult-type diffuse gliomas and subsequently identified IDH mutation status. The data were retrieved from the archives of the V.A. Almazov National Medical Research Centre (n = 31) and the N.P. Napalkov Cancer Center (n = 15) for 2021–2023 (Table 1).

Inclusion criteria:
- verified primary glial tumor;
- identified IDH mutation status;
- T2-FLAIR pulse sequence data documented in the MRI report.

Non-inclusion criteria:
- a history of previous surgery in the ROI, chemo- and radiotherapy;
- brain malformations;
- artifacts compromising interpretation of tissue transformations in the ROI.

Table 1 shows that the majority of the neoplasms were grade 4 glioblastomas, since, according to the 2021 WHO classification of tumors of the CNS, only this morphological type of tumor is characterized by the absence of IDH mutations.

The MR scans were performed with different types of tomographs at 1.5 and 3 T, so the images had to be pre-processed. MRI parameters:
- pulse sequence, plane: T2FLAIR, ax;
- slice thickness: 2–6 mm;
- field of view: 186 × 230, 199 × 220, 201 × 230, 226 × 250;
- time of repeat (TR), ms: 4,800–11,000;
- time of echo (TE), ms: 61.00–365.27.

At this study stage, we compared the effectiveness of the following raw data preprocessing techniques (transforms):
1. Normalization of image intensity distribution: to bring it to the standard normal distribution where the mean is 0 and the standard deviation is 1.
2. Image scaling (ScaleIntensity): to bring image intensity values to the predefined range (from 0 to 1).
3. Image contrast adjustment via γ-correction (AdjustContrast): to highlight structures and details crucial for the analysis.
4. Histogram normalization: to redistribute voxel intensity values for a normal (Gaussian) distribution of frequencies throughout the entire range of values.

The transforms were performed with MONAI library generic interfaces [23]. All the normalization methods were applied to each image individually. Non-normalized data were used for comparison, allowing us to evaluate the effect of preprocessing on the study results.

ROIs were segmented by a radiology expert using LevelTracing, a semi-automatic segmentation tool in 3D Slicer open-source software. The choice of this tool, grounded by the

results of our comparative effectiveness research and its operation principle, has been described previously [22]. We also used neuro-fuzzy ensembles for brain tumor segmentation[1].

The ROIs traditionally covered the entire area of the tumor lesion with hyperintense MR signal on T2-FLAIR images, including cystic and/or necrotic, hemorrhagic, and calcified components of the tumor. Such coverage is intended to significantly speed up the segmentation of the primary MR image and to standardize it to some extent by eliminating potential discrepancies in the identification of the tumor structural components due to operator-dependent variations in image segmentation.

For each ROI, 851 radiomic features were extracted: 107 original features from 7 radiomic classes and additional data obtained by discrete wavelet transforms (DWT) with a wavelet filter computing eight decompositions (HHH, HHL, HLH, HLL, LHH, LHL, LLH, LLL) per segment[2].

To convincingly demonstrate the effect of various preprocessing methods on the performance of the developed predictive model, we have selected such radiomic features that showed the best results in the previous stage of our study [22], namely:

Sphericity – a measure of the roundness of the ROI shape relative to a sphere with the smallest possible surface area, which sphericity is equal to 1 (value range is 0–1; this parameter does not reflect textural features, so it cannot be filtered out by wavelet decompositions);

Dependence Entropy – a measure of dependence variance between voxel intensity values (computed with HHH wavelet decomposition);

Dependence Non-Uniformity Normalized – a measure of the dependence variance between different grey levels throughout the image (computed with HHH wavelet decomposition);

Dependence Variance – a measure of dependence variance between the gray levels throughout the image, which quantifies the difference between a voxel intensity value and the intensity value of its neighbors (computed using HHH- and HLN wavelet decompositions);

Small Area Emphasis – incidence of small zones with the same gray level. This feature reflects texture heterogeneity by highlighting frequently occurring small areas of equal intensity. High values of this feature may indicate a more homogeneous texture of the image, whereas low values indicate complex and heterogeneous structures (computed with a wavelet decomposition) [24].

To evaluate the classification performance of our model, we used the following metrics: accuracy, recall, precision, F1 score, and AUC score.

[1]Cardoso M.J., Li W., Brown R. et al. MONAI: an open-source framework for deep learning in healthcare. 2022. URL: https://arxiv.org/pdf/2211.02701v1
[2]Radiomic Features — pyradiomics 2.2.0.post35+g8da1db7 documentation. 2016. URL: https://pyradiomics.readthedocs.io/en/latest/features.html

The dataset (46 brain MRI reports) was divided into two groups: 31 reports were used as a training sample, and 15 reports were used as a test sample. To evaluate the predictive performance of the model and given the limited input data, we performed 5-fold cross-validation of the dataset. The developed model was evaluated by each feature individually using the AUC score. This approach ensured the reliability of the metrics obtained for assessing the stability and predictive performance of the model when applied to different subsets of the input data.

To train our classification model, we used Random Forest, a decision tree ensemble algorithm, which incorporates a bagging technique to aggregate predictions from different training sets. Random Forest trains each decision tree independently on random subsets of the input data, ensuring diversity of the ensemble models and considering non-linear correlation between the features. The number of decision trees was limited to 50 to balance the variance of the model with its stability.

The null hypothesis assumed that the selected image preprocessing techniques do not affect the accuracy of IDH mutation status classification. In other words, the difference between the mean AUC values for the features extracted using different preprocessing techniques and for the unprocessed data is statistically insignificant. The alternative hypothesis states that the preprocessing techniques do affect the accuracy of IDH mutation status classification, which is presented by statistically significant differences in the mean AUC values compared to the unprocessed data.

To evaluate the reliability of the model for the study results, we used Student's t-test, which allows us to compare the distribution of quality metrics for different features (AUC) and detect statistically significant differences for this parameter. The significance level was calculated for each feature individually.

Results

Using the test sample, we calculated predictive performance values for the ROI radiomic features, which significantly correlated with IDH mutation status, according to the applied methods of source image normalization (Table 2).

For the Sphericity feature, we found no statistically significant difference between the preprocessed and unprocessed data, suggesting that the effects of different preprocessing techniques may vary depending on the feature being analyzed.

Of particular note is an experimental predictive model based on a set of radiomic features. This model demonstrated a significant improvement in classification quality due to preprocessing techniques applied ($p < 0.05$).

In this experimental model, preprocessing with the ScaleIntensity transform considering the entire set of radiomic features yielded the best result. The highest scores of feature importance in this model had dependence variance (24.3%) and dependence entropy (22.0%), as the most significant for classification. They were followed by dependence non-uniformity normalized (19.3%) and small

Table 2. Effects of image preprocessing on accuracy of IDH mutation status prediction (AUC score), *M* ± *SD* (*p*)

Radiomic feature	Unprocessed	Image intensity normalization	ScaleIntensity	AdjustContrast	Histogram normalization
Sphericity	0.645 ± 0.197	0.635 ± 0.223 (0.695)	0.660 ± 0.194 (0.713)	0.65 ± 0.177 (0.464)	0.685 ± 0.235 (0.237)
Dependence Entropy_HHH	0.59 ± 0.142	**0.76 ± 0.141* (0.042)**	0.665 ± 0.144 (0.28)	0.725 ± 0.101 (0.101)	0.585 ± 0.161 (0.325)
Dependence Non-Uniformity Normalized_HHH	0.655 ± 0.16	**0.855 ± 0.093* (0.010)**	0.770 ± 0.109 (0.153)	**0.805 ± 0.128* (0.043)**	0.630 ± 0.119 (0.843)
Dependence Variance_HHH	0.68 ± 0.184	0.670 ± 0.107 (0.589)	**0.840 ± 0.119* (0.023)**	**0.795 ± 0.141* (0.036)**	0.56 ± 0.142 (0.358)
Dependence Variance_HHH	0.355 ± 0.126	0.650 ± 0.094 (0.566)	0.535 ± 0.211 (0.572)	0.66 ± 0.051 (0.687)	**0.825 ± 0.087* (0.013)**
Small Area Emphasis_LHL	0.48 ± 0.081	0.725 ± 0.094 (0.089)	0.650 ± 0.157 (0.532)	0.665 ± 0.111 (0.536)	0.695 ± 0.187 (0.753)
All features	0.63 ± 0.088	**0.815 ± 0.058* (0.020)**	**0.845 ± 0.089* (0.005)**	**0.805 ± 0.09* (0.037)**	**0.82 ± 0.127* (0.027)**

Note. $p < 0.05$ compared to the unprocessed data.

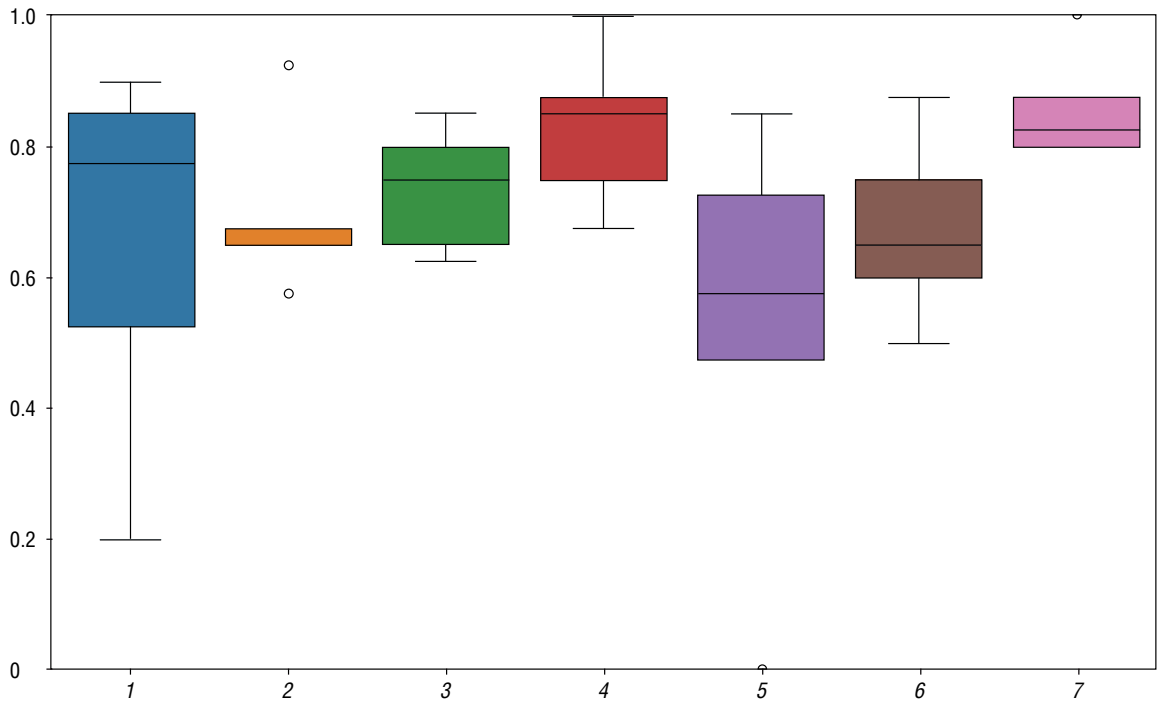

Fig. 1. Box plot displaying the results of 5-fold cross-validation of image preprocessing with the ScaleIntensity transform.
1 – Sphericity; *2* – Dependence Entropy_HHH; *3* – Dependence Non-uniformity Normalized_HHH; *4* – Dependence Variance_HHHH; *5* –Dependence Variance_HLH; *6* – Small Area Emphasis_LHL; *7* – all features.

area emphasis (18.5%). Sphericity and dependence variance had lower scores (8.2% and 7.7%, respectively); nevertheless, they contribute to classification improvement when combined with other features.

The box plot in Fig. 1 presents the spread of prognostic values for radiomic features extracted with the Scaleintensity transform (as the most effective preprocessing technique) and statistical characteristics of each subset. Classification

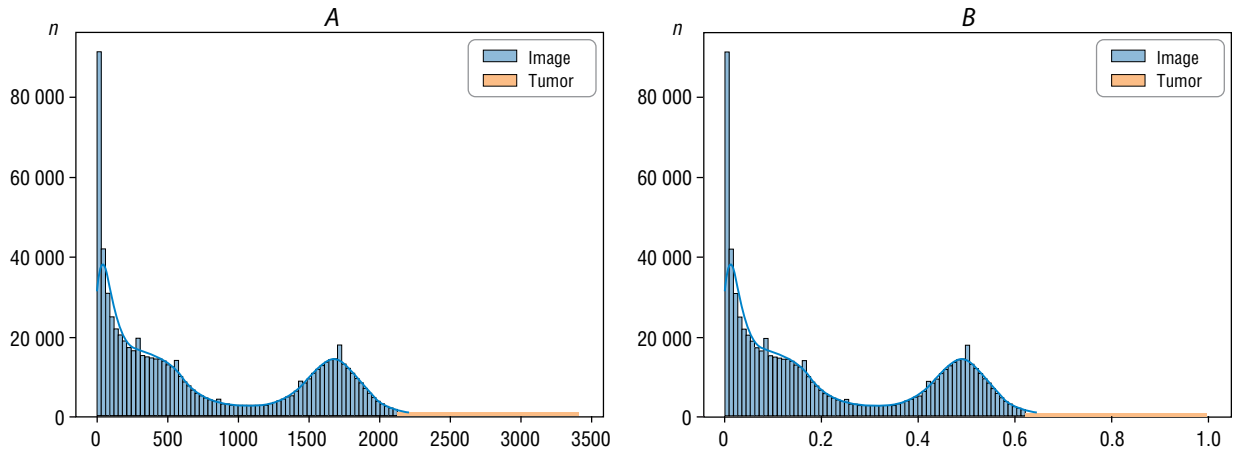

Fig. 2. Quantitative distribution of voxels with specific gray levels throughout all dataset images.
A — raw data; *B* — ScaleIntensity transformed data.

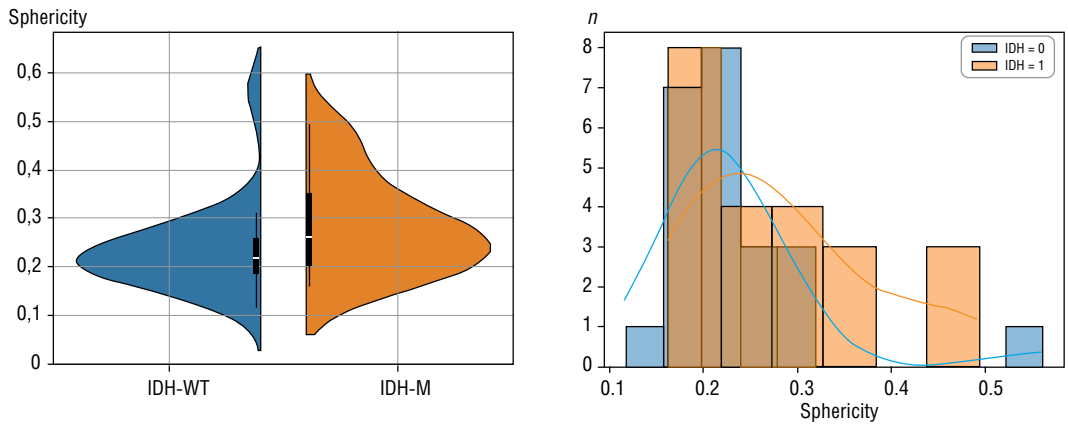

Fig. 3. Violin plot outlining sphericity values.

models considering the entire set of features demonstrate the highest predictive performance.

The ScaleIntensity transform adjusts the image intensity in the predefined range by applying the linear transformation to each element of the array. This approach allows comparing images acquired with different scanning methods.

The quantitative distribution of voxels with different gray levels across all dataset images prior to and after applying the ScaleIntensity transform is shown in Fig. 2.

Noteworthy, normalization had no effect on the sphericity value, as the sphericity formula uses only the volume and area of the segmentation zone. Differences in the AUC score for this feature can be explained by 5-fold cross-validation of the training sample, so the model was tested on five different subsamples. Distribution of the sphericity values within the entire dataset is presented in Fig. 3. A greater number of tumors with relatively high sphericity values were found in the IDH-M subgroup. The tumor with the highest sphericity value in the sample had no mutation in the IDH gene.

Figure 4 shows the ROC curve and confusion matrix for the IDH mutation status predictive model in adult-type diffuse gliomas based on the above-mentioned six radiomic features and trained with Random Forest classification, where the source images were normalized via the ScaleIntensity transform. The AUC score for the developed model is 0.845 ± 0.089, and the key metrics are accuracy 0.866; precision 0.875; recall 0.875; F1 score 0.874. According to the confusion matrix, the model produced 1 false-positive result and 1 false-negative result from the test sample of 15 reports. In other 13 cases, IDH-M and IDH-WT mutation statuses were classified correctly.

Discussion

At the previous study stage, we evaluated the predictive performance of six individual IDH mutation status predictors, extracted from ROIs in the MR scans, which were preprocessed by histogram matching and the ScaleIntensity transform, the latter yielding the best results [22]. At the current study stage, the evaluation of the predictive performance of the combined model incorporating four different preprocessing techniques showed a similar trend. Of those four tools, only AdjustContrast does not bring the signal characteristics of images to uniform ranges of predefined or mean values, as it aims to emphasize texture differences with γ-correction by augmenting or reducing the general contrast of the image.

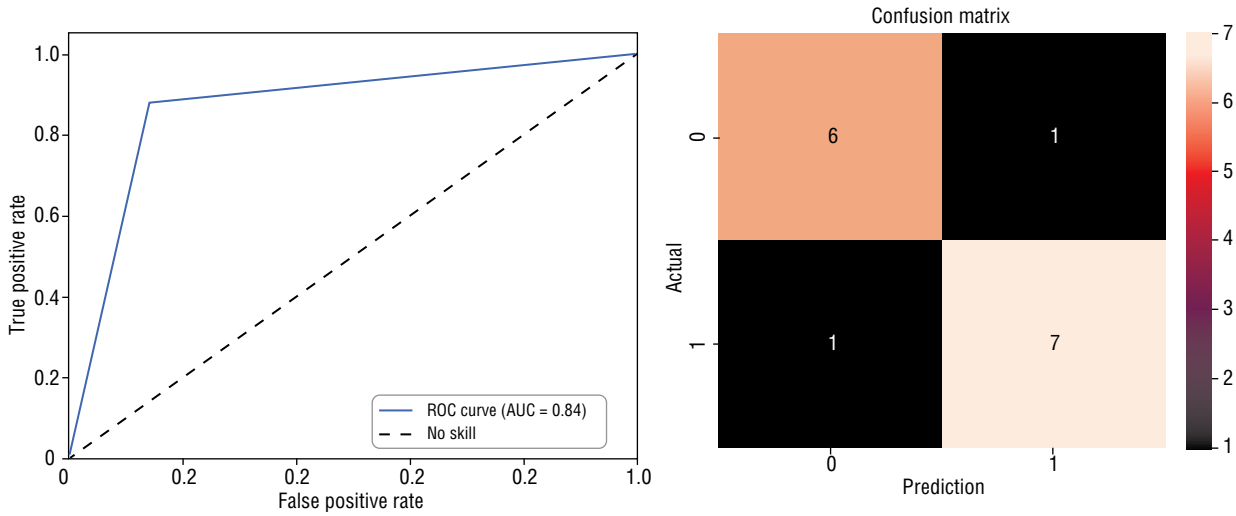

Fig. 4. ROC curve and confusion matrix of predictive model for IDH mutation status (test sample).

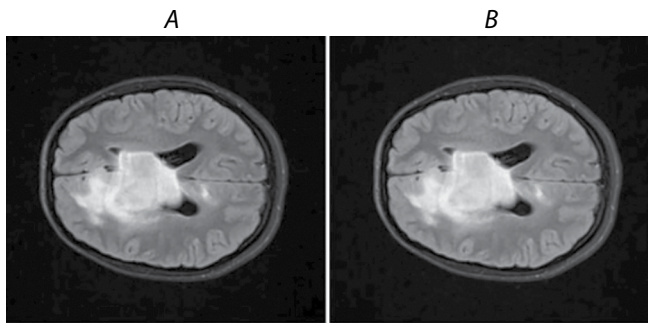

Fig. 5. Diffuse glioma (T2-FLAIR, ax).
A — raw data; *B* — AdjustContrast transformed (γ = 0.9).

At the previous study stage, we found that the majority of the radiomic predictors characterize ROI heterogeneity by gray level intensity of the voxels. Hence, the higher performance of the model built using the method of the current study stage can be associated with the contrast adjustment. Gamma (γ) value adjusts the contrast as a function: $\gamma < 1$ reduces contrast, and $\gamma > 1$ augments contrast. At the current study stage, γ was > 0.9, which means that the image contrast was slightly reduced (Fig. 5).

AdjustContrast is a crucial preprocessing technique used, for example, for computer vision tasks. Contrast adjustment improves the overall sharpness of the image, thereby enhancing the differentiation of its structural elements. This tool is primarily used for low-contrast images, where details are challenging to discern due to the insufficient difference between relatively light and dark regions[3].

The obtained result indicates that the preprocessing of source data from routine MRI based on contrast adjustment significantly improves the predictive performance of the developed model by reliably highlighting the key areas of altered MR signal, which is essential for the qualitative analysis of the MR image (see Table 2). Adjustment, almost imperceptible to the human eye, increased the model predictive performance by 17.5% compared with the model based on the raw data. Thus, γ-correction is not only critical for high-quality presentation of images and videos in different media formats (which is important considering the human-dependent perception of the image) but also a promising tool for standardization of raw medical imaging data preprocessing. However, we noticed slightly pronounced but significantly higher effectiveness of other normalization methods, which apply averaging over the signal amplitudes or bring them to a predefined range, for instance, the ScaleIntensity transform, which demonstrated the highest AUC score.

Let us compare these image preprocessing techniques. The ScaleIntensity transform is meant to uniformly increase the brightness of an image by adjusting the values of all its voxels. As a rule, the voxel values are scaled to the predefined value range by applying the linear transformation. For example, the ScaleIntensity transform can scale voxel values, which were initially in the range of 0–255, to a predefined range, often improving the quality of image interpretation without significant change of voxel-to-voxel ratio. In other words, ScaleIntensity allows us to augment

[3]Contrast Adjustment — MATLAB & Simulink.
URL: https://www.mathworks.com/help/images/contrast-adjustment.html

Table 3. ScaleIntensity vs AdjustContrast: a brief comparison of two medical imaging preprocessing techniques.

Preprocessing technique	ScaleIntensity	AdjustContrast
Effect	Uniform brightness enhancement	Greater differentiation between light and dark areas
Risk of detail loss	Low: image details are visible at any brightness level	Medium: risk of detail loss with aggressive contrast adjustment
Noise management	May reduce noise levels	May cause higher noise levels
Application	More suitable for comparative analysis	Limited to specific imaging data
Risk of clipping	Low: dynamic range preserved	High: risk of detail loss due to distorted color characteristics in too light/too light areas

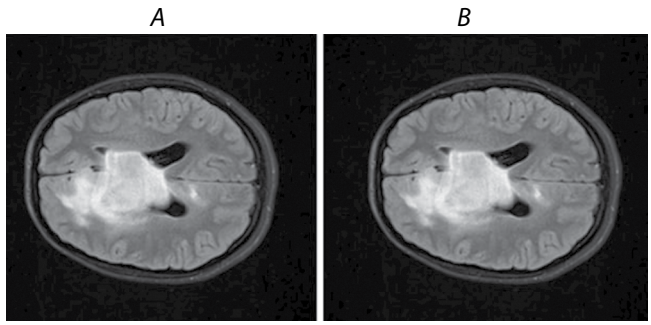

Fig. 6. Diffuse glioma (T2-FLAIR, ax).
A – raw data; *B* – ScaleIntensity transformed data.

the brightness of the image, preserving the texture of dark and light areas (Fig. 6). Uniform adjustment mitigates the risk of information loss due to critically excessive voxel intensity values.

This method also helps denoise MR images and facilitates the image structure interpretation by avoiding artifacts, which may appear with more aggressive contrast adjustment. In comparative analysis, ScaleIntensity brings a certain consistency to images with different noise levels, which is crucial for scientific imaging data analysis[4]. In turn, contrast adjustment modifies the difference between the darkest and brightest parts of the image by expanding or shrinking the range of voxel values, which improves visibility within the range by making dim areas darker and bright areas brighter. While AdjustContrast can help improve blurred image details and textures, it can also cause the risk of the detail loss in the clipping areas with too bright or dark colors. Unlike ScaleIntensity, which transforms all voxels uniformly, AdjustContrast improves the image non-uniformly by highlighting certain areas while shadowing texture in other areas, which may complicate the interpretation of the image[5].

Table 3 summarizes the main arguments, which may explain the significant difference between the predictive performance of models built using these two preprocessing techniques.

[4]Transforms — MONAI 1.4.0 Documentation. 2024.
URL: https://docs.monai.io/en/stable/transforms.html#scaleintensity
[5]Transforms — MONAI 1.4.0 Documentation. 2024.
URL: https://docs.monai.io/en/stable/transforms.html#adjustcontrast

Li et al. also demonstrated that although intensity normalization methods applied to source brain MRI images cannot completely remove the scanner effects at the radiomic feature level, they can make the neuroimaging data comparable for the subsequent analysis and increase the reliability of radiomic predictors [25]. Moreover, these methods appear to have a wider range of clinical applications, where the implementation of ComBat, a well-known image preprocessing technique, requires more computing power associated with a decrease in processing speed due to larger datasets and correspondingly more sophisticated predictive models trained on these datasets [26].

A higher number of ROIs with relatively high sphericity values in the IDH-M subgroup might be explained by less extensive areas of perifocal vasogenic edema typical for these tumor types. Such edema spreads along the gyri, giving the segmentation zones an irregular star-like shape [27, 28]. As our test sample included all morphological types of adult-type diffuse gliomas of all malignancy grades, relatively low sphericity values more often indicated more aggressive tumors, mostly represented by IDH-WT glioblastomas. The obtained result is indirectly consistent with the study of Y. Li et al., who showed that spherical disproportion (a radiomic feature characterized by minimal values for the ideal sphere) was the only independent prognostic factor positively correlated with Ki-67 proliferation index expression in lower grade gliomas [29].

The cumulative predictive performance of the model based on all six radiomic features is higher than that of the model based

on a single parameter. Therefore, our classification model based on the presence/absence of IDH mutation considers not only the severity of perifocal edema but also probably the measure of intratumor morphological heterogeneity presented by significantly higher textural ROI heterogeneity at the voxel level. We provided more detailed grounds for this assumption in one of our previous articles [22].

Given that morphological heterogeneity determines the glioma malignancy grading, our classification model, by measuring morphological heterogeneity, reflects most probably a lower or higher malignancy grade of the tumor. In its turn, numerous morphologic characteristics of high malignancy mentioned above are associated with the absence of IDH mutation, allowing the use of radiomics-based markers for indirect prediction of the IDH mutation status.

Numerous studies indicate that an astrocytic tumor, which does not fully meet the morphological criteria for higher malignancy grade but is IDH-M-free and has other specific molecular genetic characteristics, is defined as a grade 4 IDH-WT glioblastoma and should be treated according to the corresponding clinical guidelines [33–35]. Since the study samples covered tumors classified according to the updated WHO criteria, it is highly probable that some of the 24 studied IDH-WT gliomas also initially showed morphological characteristics of malignancy grade 3, which further was increased due to the IDH-M absence. So, given the diversity of adult-type diffuse gliomas in the dataset, the developed model learned to detect IDH-WT entities using the cases with less pronounced morphological characteristics of malignancy.

In many recent studies, training samples included clinical cases classified according to the 2016 WHO classification with a different IDH mutation status attributed to grade II, III diffuse astrocytomas, and grade IV glioblastomas [36]. Therefore, in some cases, the dataset was limited to specific morphologic types and malignancy grades so that the distribution of radiomic features indirectly depended only on the target variable, i.e., IDH mutation status [37, 38]. Thus, predictive models developed with this approach are of limited use for primary differential diagnosis, as they are often trained to classify IDH mutation status within a single morphological type, which is unknown to the radiologist at the time of the patient's initial examination.

Some studies disregarded IDH mutation status in the differential diagnosis of low-grade and high-grade gliomas, but in this case the radiomics-based differences between the IDH-WT and IDH-M tumor subgroups are largely associated with the minor phenotypic features, the same as in the morphologic analysis, i.e., radiomics supports the conventional methods used by radiologists [39, 40].

Conclusion

Our results demonstrate a significant impact of different MR image preprocessing methods on the accuracy of the radiomics-based IDH mutation status prediction in patients with adult-type diffuse glioma.

Based on the analysis of various tool combinations tested in routine neuroimaging and a small dataset, the combination with the highest prognostic value for pre-processing, segmentation, and classification of neuro-oncology images was found to be ScaleIntensity, LevelTracing, and Random Forest, respectively. The possible reason is that the ScaleIntensity technique can better preserve the detail and uniformity of images, which is particularly useful for comparative analysis. On the other hand, the AdjustContrast technique can improve the quality of visual interpretation, but at the cost of the structure detail loss due to non-uniformity of adjustment and the risk of clipping. At the same time, all four preprocessing techniques (ScaleIntensity, LevelTracing, Random Forest, and AdjustContrast) demonstrated similar predictive performance; hence, we should use larger datasets to train models based on these techniques and evaluate the reproducibility of the yielded results for alternative datasets.

The predictive performance of the presented model based on all six radiomic features reached the AUC score of 0.845 ± 0.089, which we will use in the further studies.

The sphericity value of the ROIs, including perifocal tissue transformations, is significantly lower in IDH-WT gliomas, as all of them have malignancy grade 4. This grade positively correlates with the severity of vasogenic edema, which is responsible for a typical irregular shape of the structural changes in tumor-associated areas.

Based on the criteria of the 2021 WHO classification of tumors of the CNS, the optimal models of IDH mutation status prediction should not be trained on samples presenting only one morphological type or a malignancy grade but rather on a sample covering various tumor types and grades to expand the model's applicability to the primary diagnostic imaging in patients with suspected adult-type diffuse glioma. Furthermore, this approach allows non-invasive exclusion of primary IDH WT glioblastoma at the initial stages of differential diagnosis.

We plan to evaluate the reproducibility of the presented model using an open-source brain MRI dataset with all types of adult-type diffuse gliomas with identified IDH mutation status and malignancy grade according to the 2021 WHO classification of tumors of the CNS. We also intend to develop a technique for color mapping of ROIs in order to facilitate visual interpretation of quantitative radiomic data.

References | Список источников

1. Ostrom QT, Patil N, Cioffi G, et al. CBTRUS statistical report: primary brain and other central nervous system tumors diagnosed in the United States in 2013–2017. *Neuro Oncol.* 2020;22(12 Suppl 2):iv1–iv96. DOI: 10.1093/neuonc/noaa200
2. Дяченко А.А. Эпидемиология и выживаемость больных первичными опухолями центральной нервной системы: популяционное исследование: дис. ... канд. мед. наук. СПб., 2014.
   Dyachenko AA. Epidemiology and survival of patients with primary tumors of the central nervous system: a population-based study. St. Peterburg, 2014. (In Russ.)
3. McKinnon C, Nandhabalan M, Murray SA, Plaha P. Glioblastoma: clinical presentation, diagnosis, and management. *BMJ*. 2021;374:n1560. DOI: 10.1136/bmj.n1560
4. Кобяков Г.Л., Бекяшев А.Х., Голанов А.В. и др. Практические рекомендации по лекарственному лечению первичных опухолей центральной нервной системы. *Злокачественные опухоли: Практические рекомендации RUSSCO #3s2*. 2018;(8):83–99. DOI: 10.18 027/2224-5057-2018-8-3s2-83-99
   Kobyakov GL, Bekyashev AH, Golanov AV, et al. Practical recommendations for drug treatment of primary tumors of the central nervous system. *Malignant tumors: Practical recommendations RUSSCO*. 2018;(8):83–99. DOI: 10.18 027/2224-5057-2018-8-3s2-83-99
5. Мацко М.В., Мацко Е.Д. Нейроонкология, 2021. Краткий анализ новой классификации Всемирной организации здравоохранения опухолей центральной нервной системы. *Вестник Санкт-Петербургского университета. Медицина.* 2022;17(2):88–100. DOI: 10.21638/spbu11.2022.202
   Matsko MV, Matsko ED. Neuro-oncology, 2021. Brief analysis of the new World Health Organization classification of tumors of the central nervous system. *Vestnik of Saint Petersburg University. Medicine*. 2022;17(2):88–100. DOI: 10.21638/spbu11.2022.202
6. Louis DN, Perry A, Wesseling P, et al. The 2021 WHO classification of tumors of the central nervous system: a summary. *Neuro Oncol*. 2021;23(8):1231–1251. DOI: 10.1093/neuonc/noab106
7. Крылов В.В., Евзиков Г.Ю., Кобяков Г.Л. Морфогенетическая характеристика глиальных опухолей у взрослых в классификациях ВОЗ 2007, 2016, 2021 гг. Изменения классификаций и их значение для клинической практики. *Нейрохирургия*. 2023;25(3):135–148. DOI: 10.17650/1683-3295-2023-25-3-135-148
   Krylov VV, Evzikov GYu, Kobyakov GL. Morphogenetic characteristics of glial tumors in adults per the WHO classifications of 2007, 2016, 2021. Changes in the classifications and their significance for clinical practice. *Russian journal of neurosurgery*. 2023;25(3):135–148. DOI: 10.17650/1683-3295-2023-25-3-135-148
8. Улитин А.Ю., Мацко М.В., Кобяков Г.Л. и др. Практические рекомендации по лекарственному лечению первичных опухолей центральной нервной системы. Практические рекомендации RUSSCO, часть 1. *Злокачественные опухоли*. 2023;13(#3s2):120–147. DOI: 10.18027/2224-5057-2023-13-3s2-1-120-147
   Ulitin AYu, Macko MV, Kobyakov GL, et al. Practical recommendations for drug treatment of primary tumors of the central nervous system. *Malignant tumors: Practical recommendations RUSSCO*. 2023;13(#3s2):120–147. DOI: 10.18027/2224-5057-2023-13-3s2-1-120-147
9. Chung CY, Pigott LE. Predicting IDH and ATRX mutations in gliomas from radiomic features with machine learning: a systematic review and meta-analysis. *Front Radiol*. 2024;4:1493824. DOI: 10.3389/fradi.2024.1493824
10. Malone H, Yang J, Hershman DL, et al. Complications following stereotactic needle biopsy of intracranial tumors. *World Neurosurg*. 2015;84(4):1084–1089. DOI: 10.1016/j.wneu.2015.05.025
11. Шашкин Ч.С., Жетписбаев Б.Б., Абдулгужина Р.М., Жуков Е.С. Стереотаксическая биопсия опухолей головного мозга. *Нейрохирургия и неврология Казахстана*. 2013;4(33):23–25.
    Shashkin ChS, Zhetpisbaev BB, Abdulguzhina RM, Zhukov ES. Stereotaxic biopsy of brain tumors. *Nejrohirurgiya i nevrologiya Kazahstana*. 2013;4(33):23–25.
12. Li Y, Qin Q, Zhang Y, Cao Y. Noninvasive determination of the IDH status of gliomas using MRI and MRI-based radiomics: impact on diagnosis and prognosis. *Curr Oncol*. 2022;29(10):6893–6907. DOI: 10.3390/curroncol29100542
13. Chang K, Bai HX, Zhou H, et al. Residual convolutional neural network for the determination of IDH status in low- and high-grade gliomas from MR imaging. *Clin Cancer Res*. 2018;24(5):1073–1081. DOI: 10.1158/1078-0432.CCR-17-2236
14. Choi Y, Nam Y, Lee YS, et al. IDH1 mutation prediction using MR-based radiomics in glioblastoma: comparison between manual and fully automated deep learning-based approach of tumor segmentation. *Eur J Radiol*. 2020;128:109031. DOI: 10.1016/j.ejrad.2020.109031
15. Hashido T, Saito S, Ishida T. Radiomics-based machine learning classification for glioma grading using diffusion- and perfusion-weighted magnetic resonance imaging. *J Comput Assist Tomogr*. 2021;45(4):606–613. DOI: 10.1097/RCT.0000000000001180
16. Lin K, Cidan W, Qi Y, Wang X. Glioma grading prediction using multiparametric magnetic resonance imaging-based radiomics combined with proton magnetic resonance spectroscopy and diffusion tensor imaging. *Med Phys*. 2022;49(7):4419–4429. DOI: 10.1002/mp.15648
17. Shen N, Lv W, Li S, et al. Noninvasive evaluation of the notch signaling pathway via radiomic signatures based on multiparametric MRI in association with biological functions of patients with glioma: a multi-institutional study. *J Magn Reson Imaging*. 2023;57(3):884–896. DOI: 10.1002/jmri.28378
18. Zhong S, Ren JX, Yu ZP, et al. Predicting glioblastoma molecular subtypes and prognosis with a multimodal model integrating convolutional neural network, radiomics, and semantics. *J Neurosurg*. 2022;139(2):305–314. DOI: 10.3171/2022.10.JNS22801
19. Rui W, Zhang S, Shi H, et al. Deep learning-assisted quantitative susceptibility mapping as a tool for grading and molecular subtyping of gliomas. *Phenomics*. 2023;3(3):243–254. DOI: 10.1007/s43657-022-00087-6
20. Guo W, She D, Xing Z, et al. Multiparametric MRI-based radiomics model for predicting H3 K27M mutant status in diffuse midline glioma: a comparative study across different sequences and machine learning techniques. *Front Oncol*. 2022;12:796583. DOI: 10.3389/fonc.2022.796583
21. Маслов Н.Е., Труфанов Г.Е., Моисеенко В.М. и др. Разработка принципов адаптации радиогеномного подхода к визуализации глиальных опухолей в рамках инициальных диагностических мероприятий. *Вестник медицинского института «РЕАВИЗ». Реабилитация, Врач и Здоровье*. 2024;14(1):168–176. DOI: 10.20340/vmi-rvz.2024.1.MIM.3
    Maslov NE, Trufanov GE, Moiseenko VM, et al. Radiogenomic approach to glial tumors imaging under conditions of initial diagnostic measures: adaptation principles development. *Bulletin of the Medical Institute "REAVIZ". Rehabilitation, Doctor and Health*. 2024;14(1):168–176. DOI: 10.20340/vmi-rvz.2024.1.MIM.3
22. Маслов Н.Е., Валенкова Д.А., Труфанов Г.Е., Моисеенко В.М. Анализ методик нормализации данных МРТ и сегментации зон интереса при рутинизации радиогеномного подхода к визуализации глиом. *Вестник Смоленской государственной медицинской академии*. 2024;(4):149–158.
    Maslov NE, Valenkova DA, Trufanov GE, Moiseenko VM. Analysis of MRI normalization techniques and ROI segmentation tools during routinization of radiogenomic approach to gliomas imaging. *Vestnik Smolenskoj gosudarstvennoj medicinskoj akademii*. 2024;(4):149–158. DOI: 10.37903/vsgma.2024.4.19

23. Valenkova D, Lyanova A, Sinitca A, et al. A fuzzy rank-based ensemble of CNN models for MRI segmentation. *Biomed Signal Proc Control*. 2025;102:107342. DOI: 10.1016/j.bspc.2024.107342
24. Antoine JP. Wavelet transforms and their applications. *Physics Today*. 2003;56(4):68–8. DOI: 10.1063/1.1580056
25. Li Y, Ammari S, Balleyguier C, et al. Impact of preprocessing and harmonization methods on the removal of scanner effects in brain MRI radiomic features. *Cancers*. 2021;13(12):3000. DOI: 10.3390/cancers13123000
26. Horng H, Singh A, Yousefi B, et al. Generalized ComBat harmonization methods for radiomic features with multi-modal distributions and multiple batch effects. Scientific Reports. 2022r;12(1):4493. DOI: 10.1038/s41598-022-08412-9
27. Hasanzadeh A, Moghaddam HS, Shakiba M, et al. The role of multimodal imaging in differentiating vasogenic from infiltrative edema: a systematic review. Indian J. Radiol. Imaging. 2023;33(4):514–521. DOI: 10.1055/s-0043-1772466
28. Min Zh, Niu Ch, Rana N, et al. Differentiation of pure vasogenic edema and tumor-infiltrated edema in patients with peritumoral edema by analyzing the relationship of axial and radial diffusivities on 3.0T MRI. *Clin. Neurol. Neurosurg.* 2013;115(8):1366–1370. DOI: 10.1016/j.clineuro.2012.12.031
29. Li Y, Qian Z, Xu K, et al. Radiomic features predict Ki-67 expression level and survival in lower grade gliomas. *J Neurooncol*. 2017 ;135(2):317–324. DOI: 10.1007/s11060-017-2576-8
30. Reuss DE, Kratz A, Sahm F, et al. Adult IDH wild type astrocytomas biologically and clinically resolve into other tumor entities. *Acta Neuropathol*. 2015;130(3):407–417. DOI: 10.1007/s00401-015-1454-8
31. Suzuki H, Aoki K, Chiba K, et al. Mutational landscape and clonal architecture in grade II and III gliomas. *Nat Genet*. 2015;47(5):458–468. DOI: 10.1038/ng.3273
32. Brat DJ, Aldape K, Colman H, et al. cIMPACT-NOW update 3: recommended diagnostic criteria for "Diffuse astrocytic glioma, IDH-wildtype, with molecular features of glioblastoma, WHO grade IV". *Acta Neuropathol*. 2018;136(5):805–810. DOI: 10.1007/s00401-018-1913-0
33. Hasselblatt M, Jaber M, Reuss D, et al. Diffuse astrocytoma, IDH-wildtype: a dissolving diagnosis. *J Neuropathol Exp Neurol*. 2018;77(6):422–425. DOI: 10.1093/jnen/nly012
34. McNamara C, Mankad K, Thust S, et al. 2021 WHO classification of tumours of the central nervous system: a review for the neuroradiologist. *Neuroradiology*. 2022;64(10):1919–1950. DOI: 10.1007/s00234-022-03008-6
35. Smith HL, Wadhwani N, Horbinski C. Major features of the 2021 WHO classification of CNS tumors. *Neurotherapeutics*. 2022;19(6):1691–1704. DOI: 10.1007/s13311-022-01249-0
36. Louis DN, Perry A, Reifenberger G, et al. The 2016 World Health Organization classification of tumors of the central nervous system: a summary. *Acta Neuropathol*. 2016;131(6):803–820. DOI: 10.1007/s00401-016-1545-1
37. Di Salle G, Tumminello L, Laino ME, et al. Accuracy of radiomics in predicting IDH mutation status in diffuse gliomas: a bivariate meta-analysis. *Radiol Artif Intell*. 2024;6(1):e220257. DOI: 10.1148/ryai.220257
38. Verduin M, Primakov S, Compter I, et al. Prognostic and predictive value of integrated qualitative and quantitative magnetic resonance imaging analysis in glioblastoma. *Cancers (Basel)*. 2021;13(4):722. DOI: 10.3390/cancers13040722
39. Zachariah RM, Priya PS, Pendem S. Classification of low- and high-grade gliomas using radiomic analysis of multiple sequences of MRI brain. *J Cancer Res Ther*. 2023;19(2):435–446. DOI: 10.4103/jcrt.jcrt_1581_22
40. Zhang Z, Xiao J, Wu S, et al. Deep convolutional radiomic features on diffusion tensor images for classification of glioma grades. *J Digit Imaging*. 2020;33(4):826–837. DOI: 10.1007/s10278-020-00322-4

Information about the authors

Nikita E. Maslov – postgraduate student, Department of radiation diagnostics and medical imaging with the clinic, Almazov National Medical Research Centre; radiologist, Department of radiation diagnostics, Saint Petersburg Clinical Scientific and Practical Center for Specialized Types of Medical Care (Oncological), Saint Petersburg, Russia, https://orcid.org/0000-0001-6098-9146
Daria A. Valenkova – engineer, Information and Methodological Center, Faculty of computer technology and informatics, Saint Petersburg Electrotechnical University «LETI», Saint Petersburg, Russia, https://orcid.org/0009-0005-3042-1476
Alexander M. Sinitca – senior researcher, Department of radio engineering systems, Saint Petersburg Electrotechnical University «LETI», Saint Petersburg, Russia, https://orcid.org/0000-0001-9869-4909
Gennadiy E. Trufanov – Dr. Sci. (Med.), Professor, Head, Department of radiation diagnostics and medical imaging with the clinic; Head, Research Institute of Radiation Diagnostics, Almazov National Medical Research Centre, Saint Petersburg, Russia, https://orcid.org/0000-0002-1611-5000
Vladimir M. Moiseenko – Corr. Member of the Russian Academy of Sciences, Professor, Director, Saint-Petersburg Clinical Scientific and Practical Center for Specialized Types of Medical Care (Oncological), Saint Petersburg, Russia, https://orcid.org/0000-0002-2246-0441
Alexander Yu. Efimtsev – Dr. Sci. (Med.), Associate Professor, Department of radiation diagnostics and medical imaging with the clinic; leading researcher, Research Institute of Radiation Diagnostics, Almazov National Medical Research Centre, Saint Petersburg, Russia, https://orcid.org/0000-0003-2249-1405
Vera V. Chernobrivtseva – Cand. Sci. (Med.), assistant, Department of radiation diagnostics and medical imaging with the clinic, Almazov National Medical Research Centre; Head, Department of radiation diagnostics, Saint Petersburg Clinical Scientific and Practical Center for Specialized Types of Medical Care (Oncological), Saint Petersburg, Russia, https://orcid.org/0000-0001-7037-177X

Authors' contribution. *Maslov N.E.* – analysis of literature data, trends; ideas, formulation and elaboration of goals and objectives; primary processing and maintenance of array research data; application of computer technologies for analysis or synthesis of research data; conducting experiments and collecting data, evidence base; development of methodology, creation of models; *Valenkova D.A.* – ideas, formulation and elaboration of goals and objectives; application of statistical, mathematical, computer techniques for the analysis and synthesis of research data; conducting experiments and collecting data, evidence base; creation of models; programming, development, software testing; *Sinitca A.M.* – application of statistical, mathematical, and computer techniques for the analysis and synthesis of research data; conducting experiments, evidence base analysis; model creation; programming, software development, and testing; *Trufanov G.E.* – ideas, formulation and elaboration of goals and objectives; management and coordination of work, planning and management of research; *Moiseenko V.M.* – analysis of literature data, trends; *Efimtsev A.Yu., Chernobrivtseva V.V.* – analysis of literature data, trends.

Информация об авторах

Маслов Никита Евгеньевич – аспирант каф. лучевой диагностики и медицинской визуализации с клиникой НМИЦ им. В.А. Алмазова; врач-рентгенолог отделения лучевой диагностики Санкт-Петербургского клинического научно-практического центра специализированных видов медицинской помощи (онкологический) им. Н.П. Напалкова, Санкт-Петербург, Россия, https://orcid.org/0000-0001-6098-9146
Валенкова Дария Андреевна – инженер информационно-методического центра факультета компьютерных технологий и информатики Санкт-Петербургского государственного электротехнического университета «ЛЭТИ», Санкт-Петербург, Россия, https://orcid.org/0009-0005-3042-1476
Синица Александр Михайлович – с. н. с. каф. радиотехнических систем Санкт-Петербургского государственного электротехнического университета «ЛЭТИ», Санкт-Петербург, Россия, https://orcid.org/0000-0001-9869-4909
Труфанов Геннадий Евгеньевич – д-р мед. наук, профессор, зав. каф. лучевой диагностики и медицинской визуализации с клиникой, заведующий НИО лучевой диагностики НМИЦ им. В.А. Алмазова, Санкт-Петербург, Россия, https://orcid.org/0000-0002-1611-5000
Моисеенко Владимир Михайлович – член-корр. РАН, профессор, директор Санкт-Петербургского клинического научно-практического центра специализированных видов медицинской помощи (онкологический) им. Н.П. Напалкова, Санкт-Петербург, Россия, https://orcid.org/0000-0002-2246-0441
Ефимцев Александр Юрьевич – д-р мед. наук, доц. каф. лучевой диагностики и медицинской визуализации с клиникой, в. н. с. НИО лучевой диагностики НМИЦ им. В.А. Алмазова, Санкт-Петербург, Россия, https://orcid.org/0000-0003-2249-1405
Чернобривцева Вера Витальевна – канд. мед. наук, ассистент каф. лучевой диагностики и медицинской визуализации с клиникой НМИЦ им. В.А. Алмазова; зав. отд. лучевой диагностики Санкт-Петербургского клинического научно-практического центра специализированных видов медицинской помощи (онкологический) им. Н.П. Напалкова, Санкт-Петербург, Россия, https://orcid.org/0000-0001-7037-177X

Вклад авторов. *Маслов Н.Е.* – анализ данных литературы, трендов; идеи, формулирование и проработка целей и задач; первичная обработка и поддержание данных исследований массива; применение компьютерных технологий для анализа и синтеза данных исследования; проведение экспериментов и сбор данных, доказательной базы; разработка методологии, создание моделей; *Валенкова Д.А.* – идеи, формулирование и проработка целей и задач; применение статистических, математических, компьютерных методик для анализа и синтеза данных исследования; проведение экспериментов и сбор данных, доказательной базы; создание моделей; программирование, разработка, тестирование программного обеспечения; *Синица А.М.* – применение статистических, математических, компьютерных методик для анализа и синтеза данных исследования; проведение экспериментов, анализ доказательной базы; создание моделей; программирование, разработка, тестирование программного обеспечения; *Труфанов Г.Е.* – идеи, формулирование и проработка целей и задач; руководство и координация работ, планирование и руководство исследованием; *Моисеенко В.М.* – анализ данных литературы, трендов; *Ефимцев А.Ю., Чернобривцева В.В.* – анализ данных литературы, трендов.